J Math Chem (2015) 53:1105–1112
DOI 10.1007/s10910-014-0441-y

ORIGINAL PAPER

Conductivities of ionic fluids in bismuth oxysulfates

Chu Rainer Kwang-Hua

Received: 14 June 2014 / Accepted: 9 November 2014 / Published online: 21 January 2015

Abstract We adopt a verified transition-state theory as well as the boundary perturbation method to calculate the ionic conductivities for a class of bismuth oxysulfates like $Bi_9SO_{16.5}$ as well as $Bi_6S_2O_{15}$. Our numerical results compared with previous experimental data of ionic conductivities of $Bi_9SO_{16.5}$ (Smirnov et al. in Solid State Ionics 156:79–84, 2003) show rather good fit. We then predict numerically the ionic conductivities for $Bi_6S_2O_{15}$ by selecting a suitable activation energy.

Keywords Bismuth oxysulfate · Activation energy · Boundary perturbation

1 Introduction

Ionic conductivity of the compounds $Bi_9SO_{16.5}$ which is a kind of bismuth oxysulfates and was synthesized from the Bi-rich part of the Bi_2O_3–SO_3 system with molar ratio range $Bi_2O_3/SO_3 = x{:}1$ ($x \equiv 4.5{:}1$) has been measured [1]. Note that at lower temperatures, a series of phase transitions takes place and Bi_2O_3 transforms into phases with low ionic conductivity. A relevant interest in oxygen-containing compounds is about the possibility of stabilization of the high temperature phase-δ-Bi_2O_3 with the defect structure of fluorite and high ionic conductivity at low temperature. A classical strategy for the improvement of ionic conductivity is doping with heterovalent cations [1].

In fact similar fluorite-related superstructures have been reported in $Bi_{14}O_{20}(SO_4)$ which was synthesized from thermal treatment of an intimate mixture of α-Bi_2O_3 and $(NH_4)_2SO_4$ in the mole ratio 1:0.14 [2]. Meanwhile quite recently a new bismuth oxysulfate $Bi_6S_2O_{15}$ nanowire which was formed from the straightforward hydrothermal reaction of Bi_2O_3 and K_2SO_4 shows promising features for application in humidity

C. R. Kwang-Hua (✉)
Centre of Transfer, No. 120-1, Section 5, Xinhai Road, Taipei 116, Taiwan, China
e-mail: ghzhu60@qq.com

sensors [3,4]. The investigation of ionic conductivity for these compounds is challenging.

However reliable theoretical conductivity equations are not always available to take into account complicated forces between the ions in complex chemicals [5,6]. Here we plan to calculate the ionic conductivity for some bismuth oxysulfates by using verified transition state approach or theory of absolute reaction [6–9]. Eyring already considered a kind of quantum tunneling which relates to the matter rearranging by surmounting a potential energy barrier [7–9]. As described by Eyring [9], mechanical loading lowers energy barriers, thus facilitating progress over the barrier by random thermal fluctuations. The Eyring model approximates the loading dependence of the barrier height as linear.

With this model we can associate the ionic transport with the momentum transfer between neighboring particle clusters on the microscopic scale and reveals the microscopic particle interaction in the relaxation of flow with dissipation (the momentum transfer depends on the activation shear volume, which is associated with the center distance between composite particles and is proportional to $k_B T/\tau_0$; k_B is the Boltzmann constant, T is temperature in Kelvin, and τ_0 a constant with the dimension of stress).

To consider the more realistic boundary conditions along the interface of a presumed microtube where ions flow, however, we will use the boundary perturbation technique [10] to handle the presumed wavy-roughness along the interface of a cross-section of the microannulus (shell-like) where ions pass through. The electric-field-driven transport is already steady and fully-developed within this wavy-rough cross-section. Thus, once we can get the velocity field and then the volume flow rate (related to flux of ions) could be directly obtained via an integration along the cross-section. To obtain the analytical and approximate solutions, here, the roughness is only introduced in the radial or transverse direction. The relevant boundary conditions along the wavy-rough surfaces will be prescribed below. We shall firstly verify our approach by comparing our numerical results for ionic conductivity of $Bi_9SO_{16.5}$ with measurements [1]. After that we then calculate ionic conductivity for $Bi_6S_2O_{15}$. Our focus is upon the reaching of higher ionic conductivity by adjusting activation energy.

2 Theoretical formulations

The standard theory on the rate of chemical reactions is the transition state theory (TST). It is generally presumed in TST that thermal fluctuations are sufficiently fast in the reactant state. To be more exact, it is assumed that before reaction occurs, thermal equilibration has already been established between the reactant and the transition states as well as among substates in the reactant state because of very fast thermal fluctuations. Thus the calculation of the rate constant is greatly simplified since we need only to calculate the transmission coefficient which describes how fast a reactant changes from the transition state to the state. We need to know also the reactant population at the transition state, but it has been determined only by the free energy of the transition state relative to the reactant state since they are in thermal equilibrium by assumption. Under this assumption, the rate constant should not depend on how fast thermal equilibration in the reactant state is attained, that is, on the thermalization time in the reactant state.

We firstly take into account a system of many (condensed) ions subjected to random thermal fluctuations (under external forcing). In thermally-activated motion, mobile ions in a many-ion system may interact with other ions even they are already in a preferred motion. The rate of deformation or strain is controlled by the rate at which thermal energy can help the system overcome their energy barriers, allowing the rest of other ions to spread.

Following Eyring's idea, the motion of ions is represented in the configuration space; on the potential surface the stable condensed particles are in the valleys, which are connected by a pass that leads through the saddle point. A condensed ion at the saddle point is in the transition (activated) state. Under the action of an applied stress the forward velocity of a flow unit is the net number of times it moves forward, multiplied by the distance it jumps. We now borrow the idea proposed before [6–9] considering the amorphous (fluid-like) characteristic of many condensed ions which is a specific microscopic model of the amorphous structure and a mechanism of deformation kinetics. With reference to this idea [6,8], this mechanism results in a shearing strain rate, considering the forward part, given by

$$\dot{\xi} = \frac{\lambda}{\lambda_1} f_r \exp(\tau V_h / 2k_B T), \tag{1}$$

where f_r is the frequency of the relaxation jump in the direction of flow (at zero stress) and has a well-known form according to the statistical theory of reactions (mentioned above), V_h is the activation volume ($= \lambda\lambda_2\lambda_3$), λ is the distance jumped on each relaxation, λ_1 is the distance between neighboring moving units in the direction normal to shear; $\lambda_2\lambda_3$ is the cross-section of the flow unit on which the shear stress acts, τ is the local applied shearing stress.

In fact, the (total) net inelastic deformation is represented as a balance between 'forward' and 'reverse' transformations [6,8,9]. We then have

$$\dot{\xi} = 2\frac{V_h}{V_m}\frac{k_B T}{h}\exp\left(\frac{-\Delta G}{k_B T}\right)\sinh\left(\frac{V_h \tau}{2k_B T}\right) \equiv \dot{\xi}_0 \sinh\left(\frac{V_h \tau}{2k_B T}\right) \tag{2}$$

where $V_m = \lambda_2\lambda_3\lambda_1$, λ_1 is the perpendicular distance between two neighboring layers of composite particles sliding past each other, and τ is the local applied stress, ΔG is the activation energy, h is the **Planck constant**, k_B is the Boltzmann constant, T is the temperature. The deformation kinetics of the chain-like composite consensed particles is envisaged as the propagation of kinks in the composite condensed particles into available holes. In order for the motion of the kink to result in a flow, it must be raised (energised) into the activated state and pass over the saddle point.

Rearranging Eq. (2) for τ, one can obtain

$$\tau = \frac{2k_B T}{V_h}\sinh^{-1}\left(\frac{\dot{\xi}}{B}\right), \tag{3}$$

which in the limit of small $(\dot{\xi}/B)$ reduces to Newton's law for viscous deformation kinetics.

We shall consider a steady transport of the many condensed ions in a wavy-rough microannulus of r_1 (mean-averaged inner radius) with the inner interface being a fixed wavy-rough surface: $r = r_1 + \epsilon \sin(k\theta + \beta)$ and r_2 (mean-averaged outer radius) with the outer interface being a fixed wavy-rough surface: $r = r_2 + \epsilon \sin(k\theta)$, where ϵ is the amplitude of the (wavy) roughness, β is the phase shift between two boundaries, and the roughness wave number: $k = 2\pi/L$ (L is the wavelength of the surface modulation in transverse direction).

Firstly, this matter (with $\tau_0 = 2k_B T/V_h$) can be expressed as $\dot{\xi} = \dot{\xi}_0 \sinh(\tau/\tau_0)$, where $\dot{\xi}$ is the shear rate, τ is the shear stress, and $\dot{\xi}_0 \equiv B$ is a function of temperature with the dimension of the shear rate. In fact, the force balance gives the shear stress at a radius r as $\tau = -[r\,\delta(\rho_i E_z)]/2$, where τ is the shear stress along the boundaries of a control volume in the transport direction (the same direction as E_z which (the only electric field) is presumed to be a constant or uniform), ρ_i is the net charge density, $|-\delta(\rho_i E_z)|$ is the net electric force along the transport or tube-axis: z-axis direction.

Introducing $\Psi = -(r_2/2\tau_0)\delta(\rho_i E_z)$ then we have $\dot{\xi} = \dot{\xi}_0 \sinh(\Psi r/r_2)$. As $\dot{\xi} = -du/dr$ (u is the velocity of the transport of the (ionic) fluid in the longitudinal (z-)direction of the presumed microannulus), after integration, we obtain

$$u = u_s + \frac{\dot{\xi}_0 r_2}{\Psi}\left[\cosh\Psi - \cosh\left(\frac{\Psi r}{r_2}\right)\right], \tag{4}$$

here, u_s is the velocity over the (inner or outer) surface of the presumed microannulus, which is determined by the boundary condition. We noticed that a general boundary condition [11] was proposed for transport over an interface as

$$\Delta u = L_s^0 \dot{\xi}\left(1 - \frac{\dot{\xi}}{\dot{\xi}_c}\right)^{-1/2}, \tag{5}$$

where Δu is the velocity jump over the interface, L_s^0 is a constant slip length, $\dot{\xi}_c$ is the critical shear rate at which the slip length diverges. The value of $\dot{\xi}_c$ is a function of the corrugation of interfacial energy.

With the boundary condition from [11], we can derive the velocity fields and electric-field-driven volume flow rates along the wavy-rough microannulus below using the verified boundary perturbation technique [10]. The wavy boundaries are prescribed as $r = r_2 + \epsilon \sin(k\theta)$ and $r = r_1 + \epsilon \sin(k\theta + \beta)$ and the presumed steady transport is along the z-direction (microannulus-axis direction).

Along the outer boundary (the same treatment below could also be applied to the inner boundary), we have $\dot{\xi} = (du)/(dn)|_{\text{on surface}}$. Here, n means the normal. Let u be expanded in ϵ: $u = u_0 + \epsilon u_1 + \epsilon^2 u_2 + \cdots$, and on the boundary, we expand $u(r_0 + \epsilon dr, \theta(=\theta_0))$ into

$$\begin{aligned} u(r,\theta)|_{(r_0+\epsilon dr,\,\theta_0)} &= u(r_0,\theta) + \epsilon\,[dr\,u_r(r_0,\theta)] + \epsilon^2\left[\frac{dr^2}{2}u_{rr}(r_0,\theta)\right] + \cdots \\ &= \left\{u_{slip} + \frac{\dot{\xi} r_2}{\Psi}\left[\cosh\Psi - \cosh\left(\frac{\Psi r}{r_2}\right)\right]\right\}\Big|_{\text{on surface}}, \quad r_0 \equiv r_1, r_2; \end{aligned} \tag{6}$$

where

$$u_{slip}|_{\text{on surface}} = L_S^0 \left\{ \dot{\xi} \left[(1 - \frac{\dot{\xi}}{\dot{\xi}_c})^{-1/2} \right] \right\} \Big|_{\text{on surface}}. \tag{7}$$

Now, on the outer interface (cf. [10])

$$\dot{\xi} = \frac{du}{dn} = \nabla u \cdot \frac{\nabla(r - r_2 - \epsilon \sin(k\theta))}{|\nabla(r - r_2 - \epsilon \sin(k\theta))|}. \tag{8}$$

Considering $L_s^0 \sim r_1, r_2 \gg \epsilon$ case, we also presume $\sinh \Psi \ll \dot{\xi}_c/\dot{\xi}_0$. With Eqs. (3) and (8), using the definition of $\dot{\xi}$, we can derive the velocity field (u) up to the second order: $u(r,\theta) = -(r_2\dot{\xi}_0/\Psi)\{\cosh(\Psi r/r_2) - \cosh\Psi\,[1 + \epsilon^2\Psi^2 \sin^2(k\theta)/(2r_2^2)] + \epsilon\Psi \sinh\Psi\, \sin(k\theta)/r_2\} + u_{slip}|_{r=r_2+\epsilon\sin(k\theta)}$. The key point is to firstly obtain the slip velocity along the boundaries or surfaces. After lengthy mathematical manipulations, we obtain the velocity fields (up to the second order) and then we can integrate them with respect to the cross-section to get the volume flow rate (Q, also up to the second order here): $Q = \int_0^{\theta_p} \int_{r_1+\epsilon\sin(k\theta)}^{r_2+\epsilon\sin(k\theta)} u(r,\theta) r dr d\theta = Q_{slip} + \epsilon\, Q_{p_0} + \epsilon^2\, Q_{p_2}$. In fact, the approximately (up to the second order) net electric-field-driven volume flow rate reads $Q \equiv Q_{out} - Q_{in}$ which is the flow within the outer (larger) wall: Q_{out} without the contributions from the flow within the inner (smaller) wall Q_{in}:

$$\begin{aligned}
Q = {} & \pi\dot{\xi}_0 \left\{ L_s^0 \left(r_2^2 - r_1^2\right) \sinh\Psi \left(1 - \frac{\sinh\Psi}{\dot{\xi}_c/\dot{\xi}_0}\right)^{-1/2} + \frac{r_2}{\Psi}\left[\left(r_2^2 - r_1^2\right)\cosh\Psi \right.\right. \\
& \left.\left. - \frac{2}{\Psi}\left(r_2^2 \sinh\Psi - r_1 r_2 \sinh\left(\Psi\frac{r_1}{r_2}\right)\right) + \frac{2r_2^2}{\Psi^2}\left(\cosh\Psi - \cosh\left(\Psi\frac{r_1}{r_2}\right)\right)\right]\right\} \\
& + \epsilon^2 \left\{ \pi\dot{\xi}_0 \left[\Psi \frac{\cosh\Psi}{4}\left(r_2 - \frac{r_1^2}{r_2}\right)\right] \right. \\
& + \frac{\pi}{4}\dot{\xi}_0 \sinh\Psi \left(1 + \frac{\sinh\Psi}{\dot{\xi}_c/\dot{\xi}_0}\right)\left(-k^2 + \Psi^2\right)\left[1 - \left(\frac{r_1}{r_2}\right)^2\right] + \frac{\pi}{2}\left[\left(u_{slip_0}\right.\right. \\
& \left. + \frac{\dot{\xi}_0 r_2}{\Psi}\cosh\Psi\right) + \dot{\xi}_0 r_2 \left(-\sinh\Psi + \frac{\cosh\Psi}{\Psi}\right) \\
& \left. + \dot{\xi}_0 \left(r_1 \sinh\left(\Psi\frac{r_1}{r_2}\right) - \frac{r_2}{\Psi}\cosh\left(\Psi\frac{r_1}{r_2}\right)\right)\right] \\
& + \pi\dot{\xi}_0 \left\{ \left[\sinh\Psi + \Psi\frac{\cosh\Psi}{r_2}\left(1 + \frac{\sinh\Psi}{\dot{\xi}_c/\dot{\xi}_0}\right)\right][r_2 - r_1\cos\beta] \right\} \\
& \left. + \frac{\pi}{4}\Psi^2\dot{\xi}_0 \frac{\cosh\Psi}{\dot{\xi}_c/\dot{\xi}_0}\left[1 - \left(\frac{r_1}{r_2}\right)^2\right]\cosh\Psi. \right.
\end{aligned} \tag{9}$$

Here,

$$u_{slip_0} = L_s^0 \dot{\xi}_0 \left[\sinh \Psi \left(1 - \frac{\sinh \Psi}{\dot{\xi}_c / \dot{\xi}_0} \right)^{-1/2} \right]. \tag{10}$$

3 Numerical results and discussion

To begin first, we check the roughness effect upon the transport characteristics because there are no available experimental data and numerical simulations for similar geometric configuration (presumed microtube with wavy corrugations in transverse direction). With a series of forcings (due to imposed electric fields): $\Psi \equiv r_2[-\delta(\rho_i E_z)]/(2\tau_0)$, we can determine the enhanced shear rates ($d\xi/dt$) due to forcings. From Eq. (8), we have (up to the first order) $d\xi/dt = (d\xi_0/dt)[\sinh \Psi + \epsilon \sin(k\theta)\Psi \cosh \Psi / r_2]$. Furthermore, if we select a (fixed) temperature, then from the expression of τ_0, we can obtain the shear stress τ corresponding to above forcings (Ψ) : $\tau = \tau_0 \sinh^{-1}[\sinh(\Psi) + \epsilon \sin(k\theta)\Psi \cosh(\Psi)/r_2]$.

The following figures are for our primary interest: Higher ionic conductivity considering electric-field-driven transport of many condensed ions (liquid-like). This can be understood from Eq. (9) or the net transport Q ($\propto \sinh \Psi$). We have the average velocity (for charge carriers): $\bar{v} = Q/A_m$ with A_m being the effective area. After this, we then have the flux of ions: $\rho_i \bar{v} = |\mathbf{J}|$ which conventionally equals to σE_z where σ is the ionic conductivity. Note that once Ψ is small then we have $\sigma \propto \bar{v} \propto \sinh \Psi \sim \Psi \propto |-\delta(\rho_i E_z)|$.

We firstly calculate the ionic conductivities for $Bi_9SO_{16.5}$ and then compare them with previous measurements (cf. figure 4 in [1]). We fix the activation energy: 1.4×10^{-19} J or 0.875 eV (while in [1] for $Bi_9SO_{16.5}$: The activation energy is equal to 0.77 and 1.1 eV (both ± 0.05 eV) in the high- and low-temperature ranges, respectively). The activation volume is temperature-dependent. Figure 1 shows that our numerical results match almost previous measurements (cf. figure 4 in [1] for $Bi_9SO_{16.5}$ ionic conductivity measured data). This good fit verifies our approach. We remid the readers that in our approach the activation energy comes from the term: $\dot{\xi}_0$ (cf. Eq. 2).

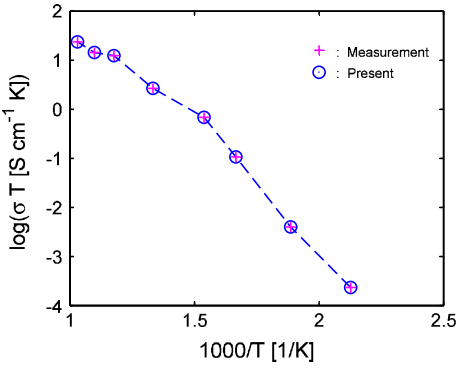

Fig. 1 Calculated ionic conductivity (σ) for $Bi_9SO_{16.5}$ compared with previous measurements (cf. figure 4 in [1]). T is the temperature (in terms of K). The activation energy is 0.875 eV ($\sim 1.4 \times 10^{-19}$ J). Both horizontal- and vertical-axis scales follow previous reported figure [1] for easy comparison

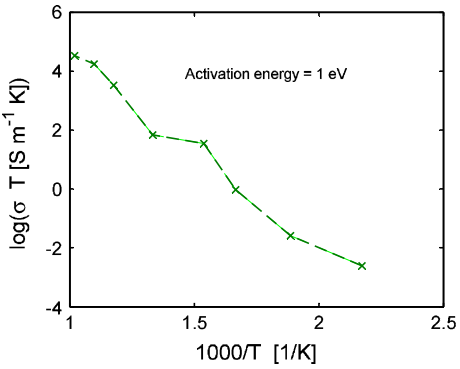

Fig. 2 Calculated ionic conductivity (σ) for $Bi_6S_2O_{15}$ [3,4]. T is the temperature. The activation energy is 1 eV ($\sim 1.6 \times 10^{-19}$ J). Both horizontal- and vertical-axis scales follow Fig. 1 but with the unit of σ : S m $^{-1} \equiv 10^{-2}$ S cm^{-1}

Furthermore, we numerically predict the ionic conductivity of $Bi_6S_2O_{15}$ [3,4] by selecting an activation energy to be 1 eV with all other parameters being almost the same as Fig. 1. The results are illustrated in Fig. 2. We can observe, since the unit of σ : S m $^{-1} \equiv 10^{-2}$ S cm^{-1}, with the selected activation energy, the ionic conductivities of $Bi_6S_2O_{15}$ are a little higher than those of $Bi_9SO_{16.5}$ within the same temperature regime.

4 Conclusion

To summarize our presentations, we have applied a verified TST approach that can calculate the ionic conductivities for a class of bismuth oxysulfates like $Bi_9SO_{16.5}$ [1] as well as $Bi_6S_2O_{15}$ [3,4]. Our numerical results compared with previous experimental data of ionic conductivities of $Bi_9SO_{16.5}$ (cf. figure 4 in [1]) show rather good fit. We shall investigate other interesting issues in the future [12].

References

1. V.I. Smirnov, V.G. Ponomareva, YuM Yukhin, N.F. Uvarov, Fluorite-related phases in the $Bi_2O_3-SO_3$ system. Solid State Ionics **156**, 79 (2003)
2. M.G. Francesconi, A.L. Kirbyshire, C. Greaves, O. Richard, G. Van Tendeloo, Synthesis and structure of $Bi_{14}O_{20}(SO_4)$: A new Bismuth Oxide Sulfate. Chem. Mater. **10**, 626 (1998)
3. Y. Zhou, G.R. Patzke, Bi_2O_3 or $Bi_6S_2O_{15}$ nanowires? The role of templating inorganic additives in nanomaterials formation. Cryst. Eng. Commun. **14**, 1161 (2012)
4. Y. Zhou, J.-D. Grunwaldt, F. Krumeich, Kb Zheng, Gr Chen, J. Stötzel, R. Frahm, G.R. Patzke, Hydrothermal synthesis of $Bi_6S_2O_{15}$ nanowires: structural, in situ EXAFS, and humidity-sensing studies. Small **6**, 1173 (2010)
5. D. Brouillette, G. Perron, J.E. Desnoyers, Effect of viscosity and volume on the specific conductivity of lithium salts in solvent mixtures. Electrochim. Acta **44**, 4721 (1999)
6. A. Chagnes, B. Carré, P. Willmann, D. Lemordant, Ion transport theory of nonaqueous electrolytes. $LiClO_4$ in g-butyrolactone: the quasi lattice approach. Electrochim. Acta **46**, 1783 (2001)
7. H. Eyring, M.S. Jhon, *Significant liquid structures* (Wiley, New York, 1969)
8. S. Glasstone, K.J. Laidler, H. Eyring, *The theory of rate processes* (McGraw-Hill, New York, 1941)
9. Yg Oh, M.S. Jhon, H. Eyring, Significant structure theory applied to liquid helium-3. Proc. Natl. Acad. Sci. (USA) **74**, 4739 (1977)
10. W.K.-H. Chu, Stokes slip flow between corrugated walls. Zeitsch. Angew. Math. Phys. **47**, 591 (1996)

11. R.K.-H. Chu, Effect of activation volume on the defect-induced anomalous electronic transport in $Rb_{0.8}Fe_2Se_2$. J. Math. Chem. **52**, 1831 (2014)
12. C.G. Jesudason, An energy interconversion principle applied in reaction dynamics for the determination of equilibrium standard states. J. Math. Chem. **39**, 201 (2006)